An integrated, multiparametric flow cytometry chip using "microfluidic drifting" based three-dimensional hydrodynamic focusing

Xiaole Mao,[1,2,a)] Ahmad Ahsan Nawaz,[1,a)] Sz-Chin Steven Lin,[1] Michael Ian Lapsley,[1] Yanhui Zhao,[1] J. Philip McCoy,[3] Wafik S. El-Deiry,[4] and Tony Jun Huang[1,2,b)]

[1]*Department of Engineering Science and Mechanics, The Pennsylvania State University, University Park, Pennsylvania 16802, USA*
[2]*Department of Bioengineering, The Pennsylvania State University, University Park, Pennsylvania 16802, USA*
[3]*National Heart, Lung, and Blood Institute at NIH, Bethesda, Maryland 20892, USA*
[4]*Penn State Hershey Cancer Institute, Hershey, Pennsylvania 17033, USA*

(Received 29 January 2012; accepted 14 March 2012; published online 20 April 2012)

In this work, we demonstrate an integrated, single-layer, miniature flow cytometry device that is capable of multi-parametric particle analysis. The device integrates both particle focusing and detection components on-chip, including a "microfluidic drifting" based three-dimensional (3D) hydrodynamic focusing component and a series of optical fibers integrated into the microfluidic architecture to facilitate on-chip detection. With this design, multiple optical signals (i.e., forward scatter, side scatter, and fluorescence) from individual particles can be simultaneously detected. Experimental results indicate that the performance of our flow cytometry chip is comparable to its bulky, expensive desktop counterpart. The integration of on-chip 3D particle focusing with on-chip multi-parametric optical detection in a single-layer, mass-producible microfluidic device presents a major step towards low-cost flow cytometry chips for point-of-care clinical diagnostics. © *2012 American Institute of Physics*. [http://dx.doi.org/10.1063/1.3701566]

I. INTRODUCTION

Flow cytometry is a powerful, high-throughput tool that can perform both quantitative and qualitative multi-parametric analyses of individual cells.[1–8] In a typical flow cytometer, the cell sample is injected through the inner tube of a coaxial channel, while sheath flows from the outer tube compress the sample flow to form a single-file stream of cells, a process known as "hydrodynamic focusing."[9–17] The focused cells pass through a laser beam, generating three types of output optical signals: forward scatter (FSC), side scatter (SSC), and fluorescence (FL). FSC is the light deflected by a cell at a small angle (2°–20°) relative to the input laser beam. The intensity of the FSC signal is indicative of the size and refractive index of the cells. SSC is the light diffused in all directions due to cellular granularity. FL is normally collected using the same optics as SSC and is later split to different detectors based on the light frequency. Each of these detection signals (FSC, SSC, and FL) is eventually processed to identify individual cells in a mixed cell population based on cell size, granularity, and various fluorescence markers.[18–23]

In the past few decades, flow cytometry has undergone remarkable advancements. It has quickly become the method of choice for a wide variety of biological studies and clinical applications, including aiding in the diagnosis of potentially fatal diseases such as leukemia,[24,25] human immunodeficiency virus (HIV),[26–28] and assessing cellular phenotypes prior to and

[a)]X. Mao and A. A. Nawaz contributed equally to this work.
[b)]Author to whom correspondence should be addressed. Electronic mail: junhuang@psu.edu.

during the course of therapeutic interventions.[28–33] The full potential of flow cytometry as a clinical diagnostic tool has yet to be realized and is still in a sustained rapid development process. Its current high cost, bulky size, mechanical complexity, and need for highly trained personnel have limited the utility of this technique. As a result, clinical flow cytometry assays have been relegated to well-equipped, centralized laboratories.[34–39] In order to overcome the limitations of conventional flow cytometry systems, researchers have made significant efforts to developing microfluidics-based miniature flow cytometry devices that could be more accessible and affordable for research laboratories and clinics.[10,12,40–53] In these approaches, the key is to develop microfluidic structures to focus particles/cells three-dimensionally.[54–65] To this end, we developed a three-dimensional (3D) hydrodynamic focusing technique called "microfluidic drifting."[10,13] By utilizing the Dean flow[65,66] in a curved microfluidic channel, "microfluidic drifting" enables 3D hydrodynamic focusing in a single-layer planar microfluidic device that can be readily fabricated via standard soft-lithography.[67] In the miniature flow cytometer we previously developed,[13] we integrated the "microfluidic drifting" based 3D hydrodynamic focusing device with an off-chip laser-induced fluorescence detection system to demonstrate a prototype miniature flow cytometer that could detect fluorescence from individual particles.

In this article, we report another major advancement: the demonstration of a single-layer flow cytometry chip that has both 3D particle focusing and multi-parametric detection components integrated on-chip. This on-chip flow cytometer employs a fiber optic-based, on-chip detection system that can be seamlessly integrated with our "microfluidic drifting" 3D particle focusing unit in a single-layer planar microfluidic device. In addition, the flow cytometer presented in this work can achieve multi-parametric detection; that is, the device detects all three of the optical output signals (FSC, SSC, and FL) from individual particles simultaneously. Our device offers a significant size reduction and a simple fabrication procedure, not to mention a reduction in required cell sample and reagent volumes, all of which contribute to the drastically reduced device cost.

II. DEVICE FUNCTION

The configuration of the flow cytometry chip is shown in Fig. 1. The device includes two major components: the fluidic module and the optical fiber-based on-chip detection module.

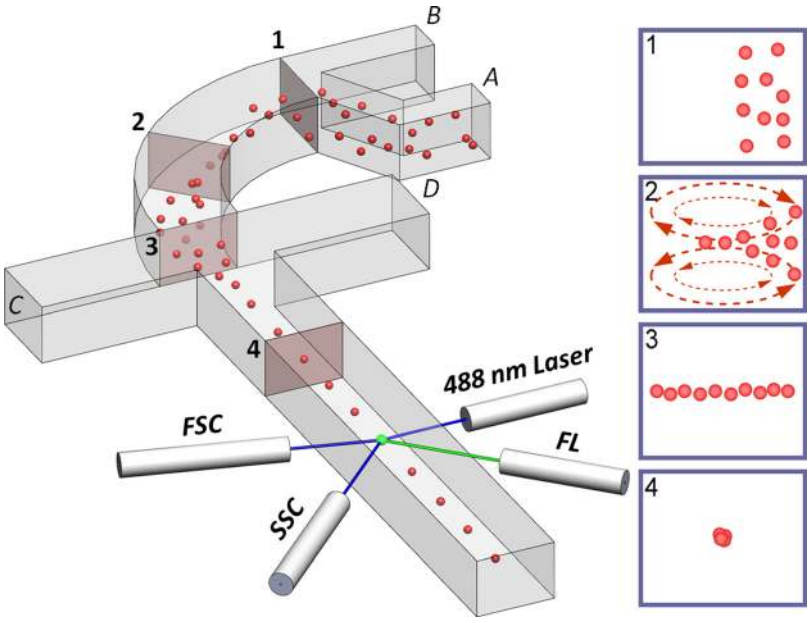

FIG. 1. Configuration of the flow cytometry chip. The fluidic channel is for 3D on-chip focusing of particles. Inlets A and B are for particles and the vertical-focusing sheath flow, respectively. Inlets C and D are for the horizontal-focusing sheath flow. The arrangement of the optical fibers is indicated in the figure.

A. Microfluidic drifting based 3D hydrodynamic focusing

The fluidic module uses "microfluidic drifting" for 3D particle focusing within a single-layer microfluidic device. The versatility of this technique lies in its simplicity and ease of fabrication. As illustrated in Fig. 1, in the first step (insets 1 to 3), the particle flow and vertical-focusing sheath flow are injected side-by-side from inlets *A* and *B*, respectively. The two flows converge and enter the 90° curve. In the curve, the induced Dean flow (inset 2), characterized by double-ring vortices in the cross-sectional plane, sweeps the particles from the top and bottom of the channel toward the center plane of the channel. This step is termed as "microfluidic drifting" and effectively focuses the flowing particles in the vertical direction (inset 3). In the second step (insets 3 to 4), the particles are pushed into a single line by the horizontal sheath flow *C* and *D*. Thus, this two-step procedure results in 3D focusing of the particles within a single-planar microfluidic channel.

The diameter of the focused stream was measured to be ~20 μm.[13] However, by optimizing the flow conditions and geometry of the microfluidic channel, the diameter of the focused particle stream can be reduced. This can be achieved by (1) decreasing the ratio between the particle flow rate and vertical-focusing sheath flow, and (2) altering the channel geometries (e.g., changing the aspect ratio of the channel or the length of the main curved channel).

B. Optical detection

As shown in Fig. 1, the fiber-based on-chip detection module includes four optical fibers: the input fiber and three detection fibers. The input fiber has a small numerical aperture (NA) and is inserted perpendicular to the channel to deliver the excitation light to the focused cell stream. The excitation light is generated by an argon laser (488 nm) and coupled to the input fiber via a fiber coupler. The three detection fibers are arranged around the main channel at different angles so that the FSC, SSC, and FL signals can be simultaneously detected. The FSC fiber is fixed at 20° from the direction of propagation of the excitation laser beam to collect forward-scattering light from the excited particles without collecting the directly transmitted light. The SSC and FL fibers are arranged 60° and 120° from the direction of propagation to collect the side-scattered light and fluorescent emission, respectively. The detection angle and the distance of the optical fibers from the main channel were optimized for detection and are similar to those in conventional flow cytometers. The collected FSC, SSC, and FL signals are transmitted through their designated fibers and a band-pass filter (488 nm filter for FSC and SSC, and 532 nm filter for FL) before they are detected by Photomultiplier tubes (PMTs).

Fig. 2(a) is an optical image taken of the integrated and assembled flow cytometry chip, whose size is comparable to a U.S. quarter. Fig. 2(b) shows a microscopic image illustrating hydrodynamic focusing due to the horizontal- and vertical-focusing sheath flows. Fig. 2(b) also shows the arrangement of the input fiber and the three detection fibers around the fluidic channel.

III. METHODS

A. Device design and fabrication

Fig. 3 shows a schematic of the fabrication procedure for the flow cytometry chip. The procedure includes four steps: (a) fabricating a polydimethylsiloxane (PDMS) layer for fluidic channels and fiber-insertion channels, (b) sealing the PDMS layer with a glass substrate, (c) inserting fluidic tubings into the microfluidic chip, and (d) inserting optical fibers into the microfluidic chip. Each inlet (vertical sheath flow and sample) is 80 μm in width. These inlets merge together forming the main channel of 167 μm width, while the side sheath flow inlets also measure 167 μm in width. The single-layered microfluidic chip was fabricated from PDMS using a standard soft lithography technique.[67–75] The master mold was made via deep reactive ion etching (DRIE) of a silicon wafer to a depth of 129 μm, thus maintaining a width to height ratio of roughly 4:3. To facilitate the removal of the cured PDMS from the mold, the surface of the mold was silanized by 1H,1H,2H,2H-perfluorooctyl-trichlorosolane vapor. We used a Harris

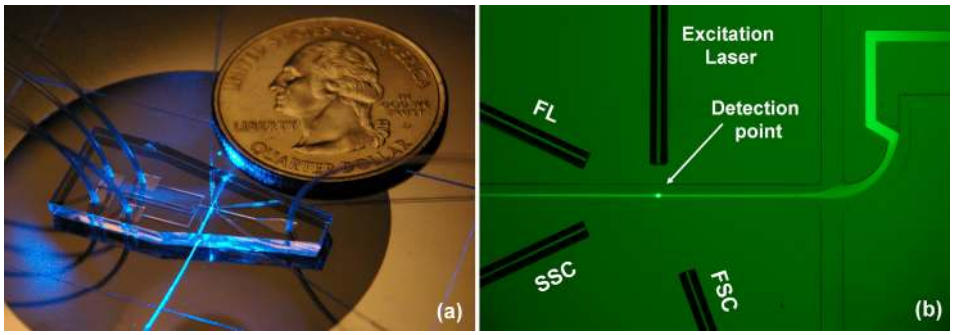

FIG. 2. (a) An assembled flow cytometry chip whose size is comparable to a U.S. quarter. The fluidic channel, optical fibers, and coupled laser beam can be clearly seen in the image. (b) A microscopic image indicating hydrodynamic focusing and the arrangement of the optical fibers. Inlet A is mixed with fluorescent dye to show the focused stream.

unicore punch (0.75 mm) to make holes for the fluid inlets and outlets in the PDMS channel and used polyethylene tubings for the inlet and outlet flows.

B. Optical methods

We used the following optical fibers in our experiments: (1) single-mode input fiber (Thorlabs S405, core diameter = 2.9 μm, cladding diameter = 125 μm, and NA = 0.14); (2) three multi-mode detection fibers (Thorlabs AFS105.125Y, core diameter = 105 μm, cladding diameter = 125 μm, and NA = 0.22). The input fiber has a relatively small NA (0.14), so that the excitation laser beam does not expand significantly (angle of light cone $\sim$16° with width of $\sim$25 μm at

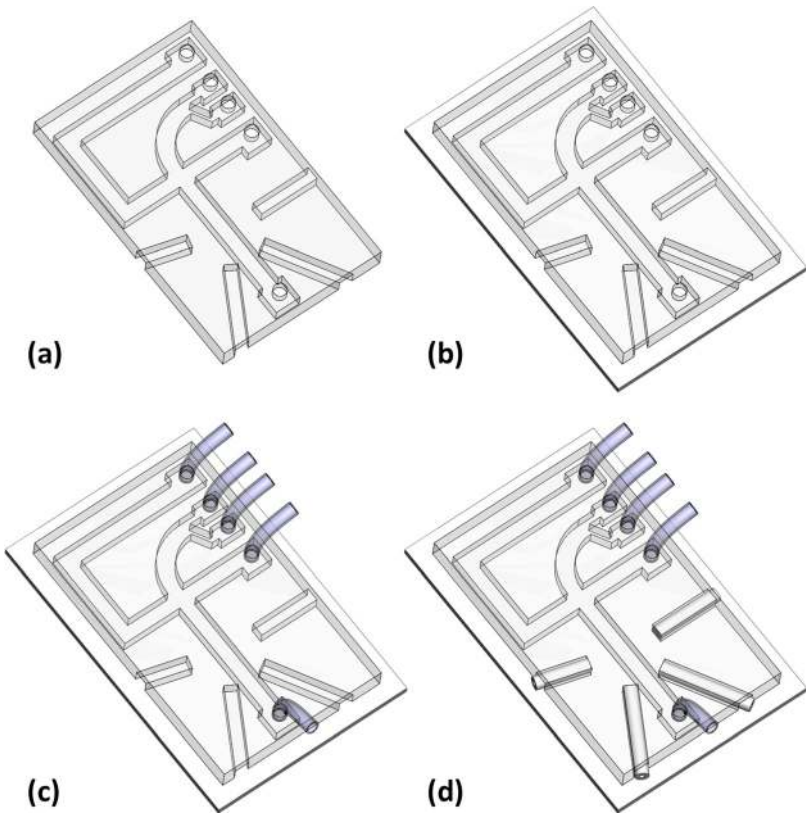

FIG. 3. Fabrication procedure of the flow cytometry chip. (a) PDMS layer for fluidic channel/fiber-insertion channel. (b) PDMS layer sealed with a glass substrate. (c) Insertion of fluidic tubings. (d) Insertion of optical fibers.

the detection point) by the time it reaches the detection point; this eliminates the need for on-chip lenses for light focusing. The NA of the three detection fibers is relatively large (NA = 0.22), so that a higher light-collection efficiency is achieved. Three PMTs (Hamamatsu 6780-20) were driven by a homemade control circuit where their gains could be individually controlled. The PMT signals were first amplified with a high-frequency amplifier (Hamamatsu C6438-01) and recorded using a digital oscilloscope (Tektronix DPO400). The height of the channel was set at 129 μm so that fibers with a diameter of 125 μm could be inserted in the fiber-insertion channels (Fig. 2(b)).

C. Sample preparation

Fluorescent (dragon green, excitation = 480 nm, and emission = 520 nm) polystyrene microparticles with two different nominal diameters of 7.32 μm (particle #1) and 15.5 μm (particle #2) were purchased from Bangs laboratories. These two sizes were carefully selected to cover the size range of human blood cells (e.g., lymphocyte ~7–8 μm and monocyte ~14–17 μm). The experiments were performed with a 1:1 mixture of particles #1 and #2. The mixed particles were diluted in a 0.01% sodium dodecyl sulfate (SDS) solution to a final concentration of $\sim 3 \times 10^6$ particles/ml and sonicated for 10 min prior to experiments to prevent particle aggregation.

IV. RESULTS AND DISCUSSIONS

A. Multi-parametric detection of fluorescent microparticles

The performance of the flow cytometry chip was characterized using commercial fluorescent microparticles. The particle solution was injected through the particle inlet *A* at a flow rate

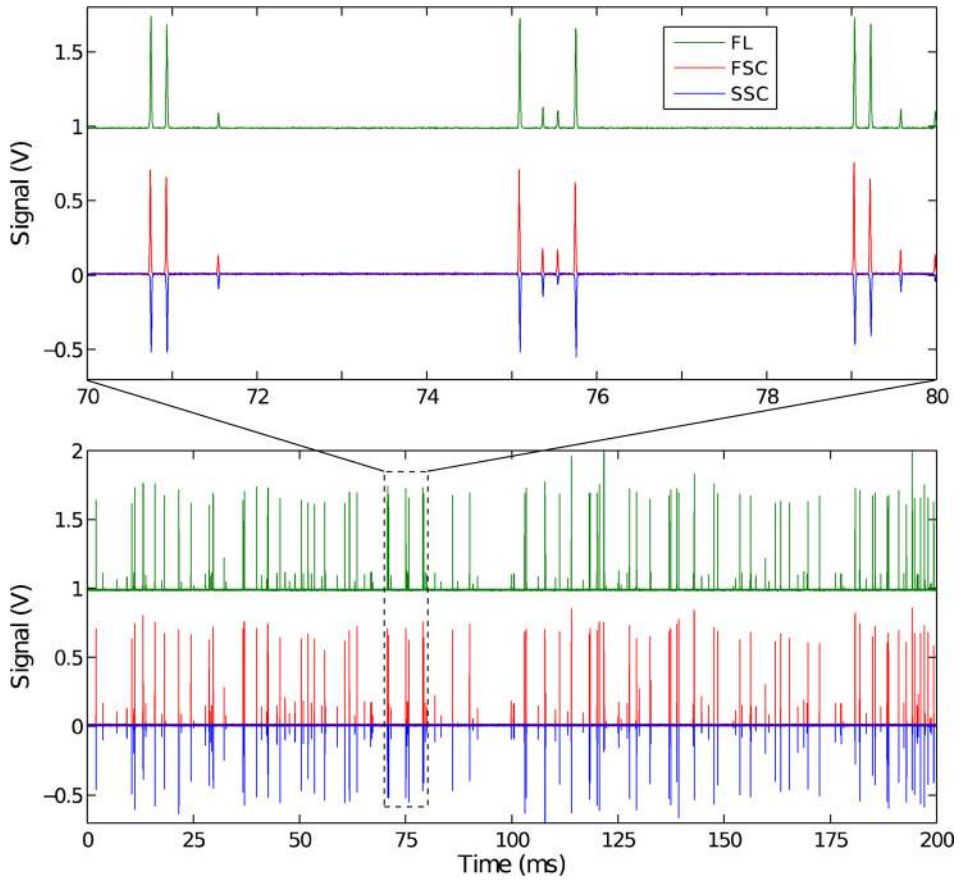

FIG. 4. Simultaneous detection of FSC, SSC, and FL signals from two types of fluorescent microparticles. The inset shows a 10 ms snapshot.

of 30.0 μl min^{-1}, whereas the vertical-focusing sheath flow rate was 370 μl min^{-1} (inlet *B*) and the horizontal-focusing sheath flow was 255 μl min^{-1} (inlets *C* and *D*). For each test, data were recorded for 4 s at a sampling rate of 2.5 MHz and analyzed with a program written in MATLAB. All three light signals were simultaneously detected and recorded. Fig. 4 shows the simultaneously detected FSC, SSC, and FL signals over 200 ms. As shown in Fig. 4, two distinctive groups of peaks, each with its own characteristic height, were identified in all three channels (FSC, FL, and SSC). Each group represents different sized fluorescent particles. An amplified view of a 10 ms interval is shown in the upper inset of Fig. 4. Despite the height differences, each group of peaks shows similar profiles with a pulse width of ~43 μs for the large particles and ~30 μs for the smaller particles. The entire 4 s of data recorded a total number of 2738 particles (685 particles s^{-1}). We also note from Fig. 4 that under the current experimental conditions, detection events are well separated, indicating a great potential to further improve the throughput of the system simply by increasing the concentration of the particles/cells.

High-efficiency PMTs (Hamamatsu 6780-20) were used in our experiments. Assuming an average linear velocity of 3.6 m/s after the side sheath fluid inlets (horizontal sheath fluid inlets) and a minimum peak-to-peak interval to be three times the peak width in order to resolve two neighboring peaks, the detection throughput of our system can be increased as high as 1 s/(3 × 43 μs) = ~8000 events s^{-1} under current flow conditions. Moreover, with optimization of design and flow conditions (e.g., curvature design and sample-to-vertical-sheath-flow ratio), the throughput of our device could reach 8000 particles s^{-1} or higher.

B. Comparison between the flow cytometry chip and a conventional flow cytometer

We compared the experimental results of our device with a commercial flow cytometry device (Beckman-Coulter FC500, unit price ~$100 000). We used 3D scatter plots of all detected events (FSC + FL + SSC) to reveal the performance of the flow cytometry device as compared to a commercial flow cytometer (Fig. 5). It can be observed that the detection events could be grouped into two distinct regions of the scatter plots for FSC vs FL vs SSC (Fig. 5(a)). The lower-region scatter (blue) represents particle #1, and the upper-region (red) represents particle #2. The results from the commercial flow cytometer with the same number of data points (2738 events) are included in Fig. 5(b) for comparison. For our flow cytometry device the peak count ratio is 43.5% for particle #1, 53.9% for the particle #2, and 2.52% for the "doublets" (aggregation of two or more small particles, represented by green dots). In contrast, for the commercial flow cytometry device, the peak count ratio is 44.7% for particle #1, 52.4% for particle #2, and 2.85% for the doublets. The results of our device match well with the experimental condition (1:1 mixing ratio), and the data from the commercial flow cytometer (Fig. 5(b)) show a similar pattern to the flow cytometry chip (Fig. 5(a)). Table I shows a comparison of coefficients of variation (CV), an indirect measure of the repeatability and precision of the flow cytometry system, for all parameters obtained from both the commercial flow cytometer and the flow

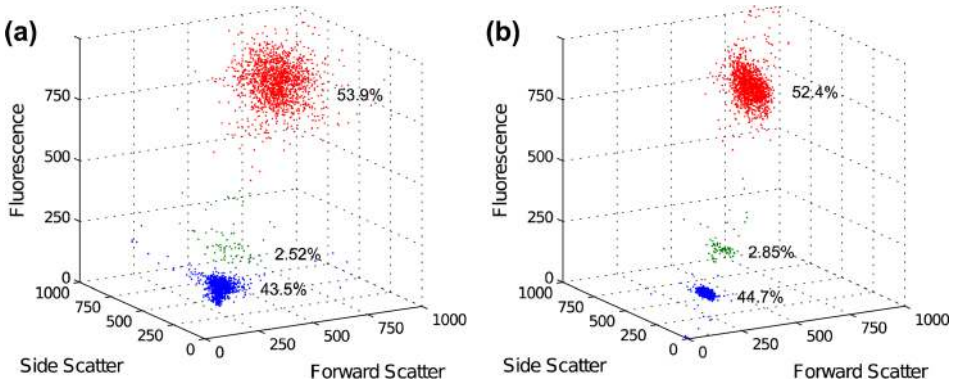

FIG. 5. Comparison of 3D scatter plots obtained from (a) the flow cytometry chip and (b) a commercial flow cytometer (Beckman-Coulter FC500).

TABLE I. Comparison of CVs of the flow cytometry chip and a commercial flow cytometer (Beckman-Coulter FC500) for the same sets of fluorescent microparticles (particles #1 and #2).

CV	Flow cytometry chip (%)	Bechman Coulter FC500 (%)
FSC, particle #1	9.1	4.2
FSC, particle #2	6.8	4.5
SSC, particle #1	17.1	13.2
SSC, particle #2	16.4	13.3
FL, particle #1	8.1	5.6
FL, particle #2	6.3	5.9

cytometry chip. The data show that the commercial flow cytometer is still slightly better than the flow cytometry chip in terms of CV. This observation is likely due to the fluctuation of particles in the focused stream in our flow cytometry chip. The width of the focused stream is around 20 μm under current flow conditions, larger than the diameters of both small and large particles. This hypothesis is supported by the fact that for both of our flow cytometry chip and the commercial one, the larger particles (particle #2, diameter = 15.5 μm) have smaller CV than the smaller particles (particle #1, diameter = 7.32 μm). Nevertheless, lower CV can be achieved by optimizing the flow conditions in our flow cytometry chip to obtain a smaller focused stream, depending on the application of future usage.

V. CONCLUSIONS

In summary, we have successfully developed and tested an integrated, multi-parametric flow cytometry chip. Our device integrates "microfluidic drifting" based on-chip 3D hydrodynamic focusing with fiber-based on-chip optical detection. The flow cytometry chip can simultaneously detect FSC, SSC, and FL signals from individual particles and was able to distinguish between the two groups of particles. Our device achieved a detection throughput of 685 particles s^{-1}. Its detection throughput can potentially be as high as 8000 particles s^{-1} under the present design in flow conditions. Compared to conventional flow cytometers, our device has significant advantages in both size and cost. With further developments, the technologies presented in this work could lead to chip-sized, low-cost flow cytometry for point-of-care clinical use. Such a flow cytometry chip will enable "decentralized" flow cytometry applications and could have a transformative impact on both fundamental biological research and clinical diagnostics.

ACKNOWLEDGMENTS

This research was supported by National Institutes of Health (NIH) Director's New Innovator Award (1DP2OD007209-01), the National Science Foundation, US Department of Agriculture (USDA/NRI), Air Force Office of Scientific Research (AFOSR), and the Penn State Center for Nanoscale Science (MRSEC). Components of this work were conducted at the Penn State node of the NSF-funded National Nanotechnology Infrastructure Network (NNIN).

[1]D. W. Inglis, J. A. Davis, T. J. Zieziulewicz, D. A. Lawrence, R. H. Austin, and J. C. Sturm, J. Immuno. Methods **329**, 151 (2008).
[2]D. W. Inglis, K. J. Morton, J. A. Davis, T. J. Zieziulewicz, D. A. Lawrence, R. H. Austin, and J. C. Sturm, Lab Chip **8**, 925 (2008).
[3]O. D. Laerum and T. Farsund, Cytometry, Part B **2**, 1 (1981).
[4]H. M. Shapiro and R. C. Leif, *Practical Flow Cytometry* (Wiley-Liss, New York, 2003).
[5]M. Brown and C. Wittwer, Clin. Chem. **46**, 1221 (2000). Available at: http://www.clinchem.org/content/46/8/1221.full.
[6]M. Rosenauer and M. J. Vellekoop, Biomicrofluidics **4**, 043005 (2010).
[7]S. H. Cho, J. M. Godin, C. H. Chen, W. Qiao, H. Lee, and Y. Lo, Biomicrofluidics **4**, 043001 (2010).
[8]N. Hashemi, J. S. Erickson, J. P. Golden, and F. S. Ligler, Biomicrofluidics **5**, 032009 (2011).
[9]M. Rosenauer, W. Buchegger, I. Finoulst, P. Verhaert, and M. Vellekoop, Microfluid. Nanofluid. **10**, 761 (2011).
[10]X. Mao, J. R. Waldeisen, and T. J. Huang, Lab Chip **7**, 1260 (2007).
[11]A. Terray and S. J. Hart, Lab Chip **10**, 1729 (2010).

[12]N. Watkins, B. M. Venkatesan, M. Toner, W. Rodriguez, and R. Bashir, Lab Chip **9**, 3177 (2009).
[13]X. Mao, S.-C. S. Lin, C. Dong, and T. J. Huang, Lab Chip **9**, 1583 (2009).
[14]R. Scott, P. Sethu, and C. K. Harnett, Rev. Sci. Instrum. **79**, 046104 (2008).
[15]C. Simonnet and A. Groisman, Appl. Phys. Lett. **87**, 114104 (2005).
[16]S. Chiavaroli, D. Newport, and B. Woulfe, Biomicrofluidics **4**, 024110 (2010).
[17]C. Huang, C. Weng, and C. P. Jen, Biomicrofluidics **5**, 044101 (2011).
[18]I. Sraj, C. D. Eggleton, R. Jimenez, E. Hoover, J. Squier, J. Chichester, and D. W. M. Marr, J. Biomed. Opt. **15**, 047010 (2010).
[19]C. Simonnet and A. Groisman, Anal. Chem. **78**, 5653 (2006).
[20]C.-C. Fu, G. Ossato, M. Long, M. A. Digman, A. Gopinathan, L. P. Lee, E. Gratton, and M. Khine, Appl. Phys. Lett. **97**, 203101 (2010).
[21]T. G. Jensen, L. B. Nielsen, and J. P. Kutter, Electrophoresis **32**, 1224 (2011).
[22]O. Laczka, J. M. Maesa, N. Godino, J. Campo, M. F. Hansen, J. P. Kutter, D. Snakenborg, F. X. Pascual, and E. Baldrich, Biosens. Bioelectron. **26**, 3633 (2011).
[23]A.-Q. Liu, Biomicrofluidics **4**, 042901 (2010).
[24]C. Dong, M. J. Slattery, B. M. Rank, and J. You, Ann. Biomed. Eng. **30**, 344 (2002).
[25]J. You, A. M. Mastro, and C. Dong, Exp. Cell Res. **248**, 160 (1999).
[26]W. R. Rodriguez, N. Christodoulides, P. N. Floriano, S. Graham, S. Mohanty, M. Dixon, M. Hsiang, T. Peter, S. Zavahir, I. Thior, D. Romanovicz, B. Bernard, A. P. Goodey, B. D. Walker, and J. T. McDevitt, PLoS Med. **2**, e182 (2005).
[27]X. Cheng, D. Irimia, M. Dixon, K. Sekine, U. Demirci, L. Zamir, R. G. Tompkins, W. Rodriguez, and M. Toner, Lab Chip **7**, 170 (2007).
[28]P. K. Dagur, A. Biancotto, L. Wei, H. N. Sen, M. Yao, W. Strober, R. B. Nussenblatt, and J. P. McCoy, Jr., J. Autoimmun. **37**(4), 319 (2011).
[29]X. Cai, G. Pacheco-Rodriguez, Q. Y. Fan, M. Haughey, L. Samsel, S. El-Chemaly, H. P. Wu, J. P. McCoy, W. K. Steagall, J. P. Lin, T. N. Darling, and J. Moss, Am. J. Respir. Crit. Care Med. **182**(11), 1410 (2010).
[30]N. A. Kentrou, N. J. Tsagarakis, K. Tzanetou, M. Damala, K. A. Papadimitriou, D. Skoumi, A. Stratigaki, N. I. Anagnostopoulos, E. Malamou-Lada, P. Athanassiadou, and G. Paterakis, Cytometry, Part B **80B**, 324 (2011).
[31]J. E. Allen, L. S. Hart, D. T. Dicker, W. Wang, and W. S. El-Deiry, Cancer Biol. Ther. **8**, 2193 (2009).
[32]J. F. Dorsey, A. Mintz, X. Tian, M. L. Dowling, J. P. Plastaras, D. T. Dicker, G. D. Kao, and W. S. El-Deiry, Mol. Cancer Ther. **8**, 3285 (2009).
[33]Y. Malka and S. Eden, Cytometry, Part A **79A**, 243 (2011).
[34]H. W. Wu, R. C. Hsu, C. C. Lin, S. M. Hwang, and G. B. Lee, Biomicrofluidics **4**, 024112 (2010).
[35]J. Gordin, C.-H. Chen, S. H. C. Cho, W. Qiao, F. Tsai, and Y.-H. Lo, J. Biophotonics **1**, 355 (2008).
[36]J.-M. Lim, S.-H. Kim, and S.-M. Yang, Microfluid. Nanofluid. **10**, 211 (2011).
[37]J. Godin, V. Lien, and Y.-H. Lo, Appl. Phys. Lett. **89**, 061106 (2006).
[38]J. Godin and Y.-H. Lo, Biomed. Opt. Express **1**, 1472 (2010).
[39]M. J. Rosenbluth, W. A. Lam, and D. A. Fletcher, Lab Chip **8**, 1062 (2008).
[40]J. Oakey, R. W. Applegate, J. E. Arellano, D. D. Carlo, S. W. Graves, and M. Toner, Anal. Chem. **82**, 3862 (2010).
[41]D. Holmes, D. Pettigrew, C. H. Reccius, J. D. Gwyer, C. van Berkel, J. Holloway, D. E. Davies, and H. Morgan, Lab Chip **9**, 2881 (2009).
[42]M. J. Kennedy, S. J. Stelick, L. G. Sayam, A. Yen, D. Erickson, and C. A. Batt, Lab Chip **11**, 1138 (2011).
[43]T. J. Kipps and D. A. Carson, in *Williams Hematology*, 7th ed., edited by E. Beutler, M. A. Lichtman, B. S. Coller, T. J. Kipps, U. Seligsohn, and J. Prchal (McGraw-Hill, Columbus, 2005), Chap. 75, p. 1031.
[44]C.-H. Lin and G.-B. Lee, J. Micromech. Microeng. **13**, 447 (2003).
[45]C. Chen, S. H. Cho, F. Tsai, A. Erten, and Y.-H. Lo, Biomed. Microdevices **11**, 1223 (2009).
[46]J. P. Golden, J. S. Kim, J. S. Erickson, L. R. Hilliard, P. B. Howell, G. P. Anderson, M. Nasir, and F. S. Ligler, Lab Chip **9**, 1942 (2009).
[47]M. J. Kennedy, S. J. Stelick, L. G. Sayam, A. Yen, D. Erickson, and C. A. Batt, Lab Chip **11**, 1138 (2011).
[48]H. Cho, J. M. Godin, C.-H. Chen, W. Qiao, H. Lee, and Y.-H. Lo, Biomicrofluidics **4**, 043001 (2010).
[49]J. Loureiro, P. Z. Andrade, S. Cardoso, C. L. da Silva, J. M. Cabral, and P. P. Freitas, Lab Chip **11**, 2255 (2011).
[50]D. Spencer and H. Morgan, Lab Chip **11**, 1234 (2011).
[51]S. C. Hur, H. T. K. Tse, and D. Di Carlo, Lab Chip **10**, 274 (2010).
[52]V. Lien, K. Zhao, Y. Berdichevsky, and Y.-H. Lo, IEEE J. Sel. Top. Quantum Electron. **11**, 827 (2005).
[53]C. Church, J. Zhu, G. Wang, T. J. Tzeng, and X. Xuan, Biomicrofluidics **3**, 044109 (2009).
[54]Z. Wu, A. Q. Liu, and K. Hjort, J. Micromech. Microeng. **17**, 1992 (2007).
[55]K. J. Liu, T. D. Rane, Y. Zhang, and T.-H. Wang, J. Am. Chem. Soc. **133**, 6898 (2011).
[56]R. Afshar, Y. Moser, T. Lehnert, and M. A. M. Gijs, Anal. Chem. **83**, 1022 (2011).
[57]J. Shi, X. Mao, D. Ahmed, A. Colletti, and T. J. Huang, Lab Chip **8**, 221 (2008).
[58]J. Shi, S. Yazdi, S.-C. S. Lin, X. Ding, I.-K. Chiang, K. Sharp, and T. J. Huang, Lab Chip **11**, 2319 (2011).
[59]C. P. Jen and W. F. Chen, Biomicrofluidics **5**, 044105 (2011).
[60]I. F. Cheng, H. C. Chang, D. Hou, and H. C. Chang, Biomicrofluidics **1**, 021503 (2007).
[61]C.-C. Chang, Z.-X. Huang, and R.-J. Yang, J. Micromech. Microeng. **17**, 1479 (2007).
[62]S. Chung, S. J. Park, J. K. Kim, C. Chung, D. C. Han, and J. K. Chang, Microsyst. Technol. **9**, 525 (2003).
[63]T. A. Lin, A. E. Hosoi, and D. J. Ehrlich, Biomicrofluidics **3**, 014101 (2009).
[64]M. G. Lee, S. Choi, and J. K. Park, Lab Chip **9**, 3155 (2009).
[65]A. A. S. Bhagat, S. S. Kuntaegowdanahalli, and I. Papautsky, Lab Chip **8**, 1906 (2008).
[66]S. S. Kuntaegowdanahalli, A. A. S. Bhagat, G. Kumar, and I. Papautsky, Lab Chip **9**, 2973 (2009).
[67]Y. Xia and G. M. Whitesides, Annu. Rev. Mater. Sci. **28**, 153 (1998).
[68]J. Shi, H. Huang, Z. Stratton, A. Lawit, Y. Huang, and T. J. Huang, Lab Chip **9**, 3354 (2009).
[69]J. Shi, D. Ahmed, X. Mao, S.-C. S. Lin, and T. J. Huang, Lab Chip **9**, 2890 (2009).
[70]X. Mao, S.-C. S. Lin, M. I. Lapsley, J. Shi, B. K. Juluri, and T. J. Huang, Lab Chip **9**, 2050 (2009).

[71]D. Ahmed, X. Mao, B. K. Juluri, and T. J. Huang, Microfluid. Nanofluid. **7**, 727 (2009).
[72]X. Mao, J. R. Waldeisen, B. K. Juluri, and T. J. Huang, Lab Chip **7**, 1303 (2007).
[73]J. Shi, D. Ahmed, X. Mao, S.-C. S. Lin, and T. J. Huang, Lab Chip **9**, 2890 (2009).
[74]D. Ahmed, X. Mao, J. Shi, B. K. Juluri, and T. J. Huang, Lab Chip **9**, 2738 (2009).
[75]X. Mao, Z. I. Stratton, A. A. Nawaz, S.-C. S. Lin, and T. J. Huang, Biomicrofluidics **4**, 043007 (2010).